# OH(OD) + CO: Measurements and an Optimized RRKM Fit

**D. M. Golden,* G. P. Smith, and A. B. McEwen†**
*SRI International, Menlo Park, California 94025*

**C.-L. Yu, B. Eiteneer, and M. Frenklach***
*Department of Mechanical Engineering, University of California, Berkeley, California 94720*

**G. L. Vaghjiani‡ and A. R. Ravishankara***
*NOAA, Boulder, Colorado 80309*

**F. P. Tully***
*Sandia National Laboratory, Livermore, California 94551*

*Received: May 4, 1998; In Final Form: July 27, 1998*

Measurements were made for the rate constant of OH + CO + He at 293 K, and OD + CO + M (M = He, Ar, $N_2$, air, $SF_6$) at 253−343 K. Results were also obtained for OH + CO in a shock tube at 1400−2600 K using OH and CO absorption. A two-channel RRKM model of these and other representative results was constructed, with five adjustable parameters. A systematic optimization method was then employed to produce the best fit of the data and provide predictive $k(T,P,D/H)$ expressions for other conditions.

## Introduction

**Past Efforts.** There have been a considerable number of studies of the reaction of OH with CO, which are discussed and referenced in a recent paper.[1] These studies, both experimental and theoretical, are motivated by the practical importance of this process. This reaction is the main source of heat in hydrocarbon combustion and the pathway for conversion of CO to $CO_2$. In the atmosphere, the reaction is a sink for CO. In the clean troposphere, it determines the daytime concentration of OH and initiates the conversion of NO to $NO_2$ via the production of $HO_2$, which in turn reacts with NO to yield OH.

This span of practical importance means that the rate constant must be accurately known as a function of temperature, pressure, and nature of possible colliders over a wide range. For use in computer models of the complex systems of combustion and the atmosphere, the goal is to represent the rate constant as a function of the above variables with a relatively simple analytical expression.

**Current Motivation.** The kinetics of the CO + OH reaction clearly are quite different from those of conventional bimolecular reactions, which are strongly sensitive to temperature and not affected by pressure. The unusual kinetic behavior of the reaction has attracted many theoretical investigations over the last two decades, including a study by Benson and co-workers.[2] It is now understood that, unlike ordinary bimolecular reactions, the reaction actually proceeds through the formation of an adduct:[1−6]

**SCHEME 1**

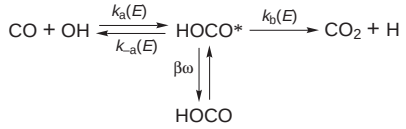


where HOCO* denotes the energized HOCO adduct, $k_a(E)$, $k_{-a}(E)$, and $k_b(E)$ are the energy-dependent rate coefficients of the elementary reaction steps, and $\beta$ and $\omega$ are the collision efficiency and collision frequency, respectively, of bath gases with the species HOCO*. (The rate constants are also dependent on the angular momentum and should be written as $k(E,J)$. The notation is simplified herein.)

The reaction mechanism given in Scheme 1 indicates that the oxidation of CO by OH may proceed as association reaction (assn) or chemical activation process (ca):[6]

$$\mathrm{CO + OH \rightarrow HOCO} \quad \text{(assn)}$$
$$\rightarrow \mathrm{CO_2 + H} \quad \text{(ca)}$$

The overall rate coefficient of the CO + OH reaction is a combination of reactions (assn and ca) (i.e., $k_{CO+OH} = k^{assn} + k^{ca.}$). The association reaction represents the case where the energized HOCO* adduct is stabilized by the bath gas to form thermalized HOCO, while in the chemical activation reaction, the energized HOCO* decomposes to produce $CO_2$ and H. The two reactions compete with each other and the back decomposition to OH and CO, in the consumption of HOCO*. At extremely high pressures, the association reaction dominates, since all the HOCO* adducts are deactivated, whereas the chemical activation reaction is the main channel for reactant

* Corresponding authors.
† Present address: Covalent Associates, Woburn, MA 01801.
‡ Present address: Phillips Laboratory, Edwards AFB, CA 93524.

10.1021/jp982110m CCC: $15.00 
Published on Web 09/12/1998

consumption at extremely low pressures. Such processes are typically discussed in the language of unimolecular rate theory.[6]

For the association reaction, using the Lindemann formulation, $k$ may be written:

$$k_{bi}^{assn} = \frac{k\beta\omega}{k_{-a} + k_b + \beta\omega}$$

$$P_r^{assn} = \frac{\beta\omega}{k_{-a} + k_b}$$

where $P_r^{assn}$ is the reduced pressure defined by Troe[7] as the low-pressure limit divided by the high-pressure limit.

The reduced rate constant is defined by

$$k_r^{assn} \equiv \frac{k_{bi}^{assn}}{k_{bi}^{assn,\infty}} = \frac{\beta\omega}{k_{-a} + k_b + \beta\omega} = \frac{P_r^{assn}}{1 + P_r^{assn}}$$

Considering the energy dependence of the rate parameters

$$k_{bi}^{assn} = K_{HOCO}\beta\omega\left\langle \frac{k_{-a}(E)}{k_{-1}(E) + k_b(E) + \beta\omega}\right\rangle_B$$

where $\langle\ \rangle_B$ signifies averaging with respect to the Boltzmann distribution.

$$K_{HOCO} = \frac{[HOCO]_{eq}}{[HO]_{eq}[CO]_{eq}}$$

Thus,

$$k_r^{assn} = \frac{P_r^{assn}}{1 + P_r^{assn}}(F^{assn})$$

where $F^{assn} = (F_c^{assn})^x$ and $x = [1 + (\log P_r)^2]^{-1}$. $F_c^{assn}$ is the value of $(F^{assn})^x$ when $P_r$ is unity (i.e., $F_c^{assn} = 2\, k_{bi}^{assn}[P_r = 1]/k_\infty^{assn}$).

For the chemical activation process, the Lindemann mechanism yields

$$k_{bi}^{ca} = \frac{k_a k_b}{k_{-a} + k_b + \beta\omega}$$

$$P_r^{ca} = \frac{\beta\omega}{k_{-a} + k_b}$$

$$k_r^{ca} = \frac{\beta\omega}{k_{-a} + k_b + \beta\omega}$$

which are the same as for the association process. Again, the actual expression is

$$k_{bi}^{ca} = K_{HOCO}\left\langle \frac{k_{-a}(E)k_b(E)}{k_{-a}(E) + k_b(E) + \beta\omega}\right\rangle_B$$

$$k_r^{ca} = \frac{P_r^{ca}}{1 + P_r^{ca}}(F_c^{ca})^x$$

Notice that for the chemical activation case, the low-pressure limit of the bimolecular rate constant is independent of pressure, while the high-pressure limiting bimolecular rate constant is best expressed as a first-order constant by multiplying by the pressure.

The rate constant, $k_c$, for production of H (and/or) $CO_2$ is just the chemical activation rate constant, $k^{ca}$, if HOCO does not thermally decompose.

$$k_c = \frac{1}{[HO][CO]}\frac{d[H]}{dt} = k_{bi}^{ca}$$

The goal is to represent the reaction of HO + CO over a wide range of temperature, pressure, and colliding gases.

Some of the authors have been previously involved in presenting simple expressions for the rate constant of this system for use in modeling.[6] These theoretically based semiempirical parametrizations, and some more recent ones developed by Troe and co-workers,[1] do a reasonable job of representing the data over wide ranges of conditions. However, the new data presented herein allow the refinement of these expressions. This paper contains reports on experimental investigations that help to improve the ability to model this system. High-precision data for the pressure dependence of the reaction in He at 293 K and the pressure dependence of the deuterated analogue at several temperatures and with several collider gases is presented. Data are also presented for the system at high temperatures ($1400 < T/K < 2600$).

RRKM theory is used to simulate the rate constants $k_{-a}$ and $k_b$ and form a sound basis for interpreting the measurements and providing the extrapolation expressions. A solution mapping technique[8−10] is used to describe the effects of the parameters of the potential energy surface (PES) on the results of the RRKM calculations. Starting with an ab initio computation,[11] certain limited details of the PES are allowed to vary within reasonable bounds. The values of these parameters are then optimized with respect to the large database now available for this reaction system. This method systematically searches for the best consistent RRKM fit to the data and is particularly useful when many results are available and the theory is especially sensitive to many parameters.

## Experiments

**OH + CO in He at 293 K.** At Sandia National Laboratory, a laser photolysis/CW laser-induced fluorescence technique measured absolute rate coefficients for the reaction between OH and CO at 293 K as a function of helium buffer-gas pressure. This technique and its application to OH-kinetics studies has been previously described,[12,13] and only a brief summary is given. OH forms from the fast reaction of $O(^1D)$ with $H_2O$ following pulsed 193 nm laser photolysis of $N_2O$. Following initiation of the reaction, time-resolved OH concentration profiles are measured as a function of the reactant CO number density using laser-induced fluorescence. The $R_1(3)$ line in the (0,0)-band of the $A^2\Sigma^+ - X^2\Pi$ OH transition is selectively excited with a <25 MHz bandwidth, CW, single-mode, intracavity-doubled, ring dye laser operating near 307 nm. The [OH] decay profiles are obtained by averaging the signal from 500 to 3000 excimer-laser pulses.

The chemicals used in this study have the following stated purities: He (99.9999%), $N_2O$ (99.99%), $H_2O$ (HPLC organic-free reagent grade), and CO (99.99%). To remove any metal−carbonyl compounds formed in the CO gas cylinder, the CO was passed through several cryogenic traps (195 K, 77 K) prior to its use in mixture preparation.

All experiments were carried out under pseudo-first-order kinetic conditions with $[OH]_0 \ll [CO]$. [CO] was varied from $(0-3) \times 10^{15}$ molecules $cm^{-3}$ and [He] from $(0.82-28.5) \times 10^{18}$ molecules $cm^{-3}$. Initial OH concentrations ranged from

**TABLE 1: Experimental Conditions and Results Used in the Optimization of the High-Temperature Experiments**

| $T_5$ (K) | $C_5 \times 10^6$ (mol cm$^{-3}$) | $P_5$ (atm) | CO | | | OH | | | $k_{R1b}/10^{11}$ (cm$^3$ mol$^{-1}$ s$^{-1}$) |
|---|---|---|---|---|---|---|---|---|---|
| | | | $t_{1/4}$ ($\mu$s) | $t_{1/2}$ ($\mu$s) | $t_{3/4}$ ($\mu$s) | $t_{1/4}$ ($\mu$s) | $t_{1/2}$ ($\mu$s) | $t_{3/4}$ ($\mu$s) | |
| Series A: 4.0% $H_2$−0.5% O2−3.0% $CO_2$−Ar | | | | | | | | | |
| 1709 | 15.76 | 2.21 | 97.1 | 122.6 | 159.1 | 70.1 | 80.0 | 105.8 | 4.5 |
| 1882 | 15.78 | 2.44 | 50.2 | 64.3 | 84.4 | 45.5 | 53.7 | 63.9 | 5.0 |
| 2097 | 12.57 | 2.16 | 36.4 | 45.3 | 57.7 | 32.4 | 38.6 | 45.8 | 5.8 |
| 2324 | 8.41 | 1.61 | 33.4 | 42.5 | 53.4 | 32.0 | 37.5 | 44.8 | 6.4 |
| Series B: 2.0% $H_2$−0.5% $O_2$−5.0% $CO_2$−Ar | | | | | | | | | |
| 1617 | 16.03 | 2.13 | 112.9 | 135.3 | 167.1 | 99.2 | 108.6 | 118.9 | 3.7 |
| 1819 | 20.99 | 3.13 | 45.8 | 54.5 | 65.6 | 40.9 | 45.2 | 49.8 | 4.7 |
| 1999 | 10.66 | 1.75 | 54.5 | 65.2 | 78.8 | 51.5 | 57.5 | 63.1 | 5.5 |
| 2198 | 10.62 | 1.92 | 36.9 | 43.4 | 53.8 | 35.6 | 39.7 | 43.4 | 5.8 |
| 2325 | 10.54 | 2.01 | 28.8 | 65.2 | 41.1 | 30.0 | 33.8 | 37.1 | 7.1 |
| Series C: 2.0% $H_2$−0.5% $O_2$−7.0% $CO_2$−Ar | | | | | | | | | |
| 1817 | 10.63 | 1.55 | 87.5 | 103.0 | 125.9 | 73.4 | 80.8 | 87.9 | 4.0 |
| 2218 | 9.08 | 1.68 | 39.6 | 46.6 | 57.6 | 35.5 | 40.0 | 43.9 | 5.3 |
| 2469 | 8.01 | 1.62 | 28.1 | 34.2 | 41.4 | 28.7 | 32.6 | 36.0 | 6.5 |
| Series D: 2.0% $H_2$−1.0% $O_2$−5.0% $CO_2$−Ar | | | | | | | | | |
| 1944 | 15.78 | 2.52 | 33.8 | 40.0 | 50.6 | 26.2 | 28.6 | 30.8 | 4.6 |
| 2165 | 15.76 | 2.80 | 21.3 | 24.7 | 30.5 | 16.6 | 18.3 | 19.9 | 6.2 |
| Series E: 2.0% $H_2$−2.0% $O_2$−7.0% $CO_2$−Ar | | | | | | | | | |
| 1427 | 13.98 | 1.64 | 103.2 | 123.1 | 159.4 | 77.4 | 82.8 | 89.0 | 3.5 |
| 1672 | 15.88 | 2.18 | 43.7 | 55.3 | 68.1 | 30.7 | 33.4 | 35.7 | 3.9 |
| 1884 | 10.79 | 1.67 | 34.6 | 42.5 | 56.0 | 26.1 | 28.9 | 30.9 | 4.7 |
| 1975 | 14.12 | 2.29 | 23.4 | 29.7 | 37.2 | 16.3 | 17.9 | 19.3 | 4.7 |
| 2253 | 10.81 | 2.00 | 17.8 | 21.2 | 27.5 | 12.4 | 13.7 | 15.0 | 6.2 |

(1−5) × $10^{10}$ molecules cm$^{-3}$, with factor of 3 variations in [$N_2O$], [$H_2O$], and the photodissociation flux having no effect on the measured kinetics. Diffusion-corrected decay constants $k' = k$[CO] were extracted from the measured [OH] profiles and effective bimolecular rate coefficients, $k$, were determined from the slope of the least-squares straight line through the ($k'$[CO]) data points. One set of such experiments was performed at each helium buffer-gas pressure.

Results are discussed in the next section. A complete table of data can be found as Supporting Information.

**OD + CO.** At the NOAA Aeronomy Laboratory, a pulsed photolysis−pulsed laser induced fluorescence apparatus was used to measure the rate coefficients for the reaction of OD + CO as a function of temperature in He, Ar, $N_2$, air, and $SF_6$. This apparatus is described elsewhere.[14] The concentration of CO flowing through the reactor was determined by measuring gas flow rates and pressure, using calibrated mass flow transducers and an absolute capacitance manometer, respectively.

In all the experiments, except those performed with air as the buffer gas, OD radicals were generated by flash photolysis of $D_2O$ in the wavelength range between 165 nm (quartz cutoff) and 181 nm ($D_2O$ absorption cutoff) using a xenon flash lamp. The output of the xenon flash lamp (∼10 ns duration) was weakly focused into the reaction zone using a $MgF_2$ lens. For experiments with air, OD was generated by pulsed laser photolysis of $D_2O_2$ at 248 nm. In this case, the excimer laser output (∼20 ns duration) was passed through the reactor unfocused.

The reagents used in the present study had the following stated purities: $D_2O$ (99.8 atom % D) supplied by Merck Sharp and Dohme, Canada. $D_2O_2$ (30% in $D_2O$) supplied by Icon Services Inc. Synthetic air (impurities of less than 2 ppm hydrocarbons) and CO (>99.9%) both supplied by Matheson Gas Products; $N_2$ (>99.998%) supplied by Union Carbide; He (>99.9996%) supplied by U. S. Bureau of Mines; and Ar (>99.999%) and $SF_6$(>99.6%) both supplied by Scientific Gas Products. All the reagents, except CO, were used as supplied. CO passed through a quartz wool packed tube heated to 500 K and through a Pyrex trap maintained at 197 °C to remove carbonyl impurities.

As with the Sandia work, the kinetics of the reaction OD + CO + M → products were studied under pseudo-first-order conditions in [OD]. In a series of experiments, data were obtained at a given temperature and constant pressure of the buffer gas M for varying concentrations of CO. [CO] ranged from 5 × $10^{15}$ to 1 × $10^{17}$ molecules cm$^{-3}$. The pseudo-first-order decay coefficient, $k'_D$, was evaluated from the plots of the logarithm of the fluorescence signal versus delay time. The second-order rate coefficient, $k_D$, was evaluated from the slope of the linear plot of $k'_D$ versus [CO]. Weighted linear least-squares fitting routines were used to calculate $k'_D$ and $k_D$. In the present study, the measured $k'_D$ ranged from ∼12 to ∼20 000 s$^{-1}$ (smallest $k'_D$ in the presence of CO was ∼1000 s$^{-1}$, and the first-order loss was typically between 12 and 50 s$^{-1}$). At a given temperature, $k_D$ was measured at various pressures of the buffer gas M; typically the pressure ranged from 16.7 to 606 Torr. A table of supporting information lists the values of $k_D$ determined in the present study over this pressure range for the five different buffer gases used: $SF_6$, $N_2$, Air, Ar, and He, at four different temperatures 253, 278, 298, and 343 K. Results are presented in the next section.

A series of systematic checks showed that the observed rate coefficients were not affected to any significant extent by possible secondary chemistry taking place in the reaction zone. A change in the linear flow velocity of the gas mixture at the reaction zone in the range 2−20 cm s$^{-1}$ had no effect on the rate coefficient. This indicated that the "slow flow" condition of the present study was adequate to ensure that no significant accumulation of reaction products from previous photolytic pulses was taking place. The photolysis energy and the precursor concentration (typically 2 × $10^{15}$ molecules cm$^{-3}$) were altered so as to vary the initial OD concentration from 1 × $10^{10}$ to 1 × $10^{11}$ molecules cm$^{-3}$, with no observable effect on the measured rate coefficient. The errors quoted in the Supporting Information are 1$\sigma$ and refer only to the precision

of the fit in $k'_D$ versus [CO] plots. The overall errors in the values of $k_D$ are determined by precision, uncertainty in [CO], and any inherent systematic errors in the experimental procedures. The latter is believed, of course, to be negligible, and the estimated uncertainty of the $k_D$ determination is less than 15%.

**OH + CO from 1400 to 2600 K.** The high-temperature experiments were performed on the reverse H + $CO_2$ reaction in a conventional 8.26 cm diameter stainless steel shock tube and are as described previously.[15] Incident shock velocities were measured with 4 PCB 482A piezoelectric pressure transducers mounted flush on the shock-tube wall with 25.4 cm spacing. A fourth transducer was mounted 1.27 cm from the endplate of the 4.9 m long driven section, the location of the laser absorption measurements. Reflected shock temperatures (0.35%) and pressures (0.09%) were calculated from the time measurements of the shock velocities (0.5 $\mu$s).

CO and OH profiles were followed by laser absorption, with a time resolution of 0.5 $\mu$s. The OH concentration was measured by a frequency doubled, actively stabilized Coherent CR-699-21 ring dye laser, tuned to the center of the $P_1$5 line of the A−X (0,0) transition at 310.123 nm (line width 2 MHz). Calibration followed the procedure of Yuan et al.[16] in shock-heated mixtures of $H_2-O_2-(CO_2)-$Ar, resulting in the expression $\epsilon_{OH} = (1.65 \pm 0.17) \times 10^{-17} - (1.00 \pm 0.35) \times 10^{-14}/T$ cm$^2$/molecule. A CW CO laser tuned to the 2-1 P(10) or 3-2 P(10) line measured the CO absorption on two vibrational levels, using a 0.25 m monochromator with an amplified, cooled InSb detector. Calibration of the Voight profile expression for the gain equation was performed in shock mixtures of 0.1−0.5% CO in Ar at 1450−2370 K and 1.3−2.6 atm after vibrational equilibration. Measurements of CO using the 3-2 line required calibrated corrections of 15% due to absorption by $CO_2$. Time zero for the kinetics is defined as 1.0 $\mu$s after the peak of the laser schlieren signal that indicates the arrival of the reflected shock wave.

Five mixtures of hydrogen−oxygen−carbon dioxide diluted in argon were used in the course of this study, with stated purity levels of 99.99%, 99.999%, 99.999%, and 99.9999%, respectively. The maximum uncertainty in manometrically prepared final reactant concentrations was about 3%. The mixtures were chosen as a result of an experimental design that involved computer modeling of the system coupled to a sensitivity analysis, using the GRI-Mech 1.2 mechanism.[17] This analysis indicated that the CO profiles were overwhelmingly sensitive to the title reaction. The OH profiles also showed strong sensitivity to the reaction H + $O_2 \rightarrow$ OH + O (a) and important sensitivity to the reactions O + $H_2 \rightarrow$ OH + O (b), OH + $H_2 \rightarrow$ $H_2O$ + H (c), and OH + OH $\rightarrow$ $H_2O$ + O (d). Table 1 summarizes the mixture compositions and some selected experiments and the measured characteristic times of both CO and OH profiles The characteristic times in Table 1 used to determine the rate constants were those corresponding to $^1/_4$, $^1/_2$, and $^3/_4$ of the maximum concentrations.

Rate constants can be extracted from the CO data in a relatively straightforward manner, given the lack of sensitivity to other processes. However, given the sensitivity of the OH signal to the above four reactions, solution mapping techniques[8−10] were used to extract a value for the rate constant of interest using both the CO and OH data. By using the time data rather than concentration results, any uncertainty in the absorption coefficients has little effect on the rate constant determinations.

The experimental observables $\Delta t$, the difference between $t_{3/4}$ and $t_{1/4}$ in Table 1, were simulated using the chemical mechanism mentioned earlier. In this mechanism, values of the five sensitive quantities, the four interfering rate constants (a)−(d) above, and the rate constant of interest, $k_{ca}$, were assigned values and uncertainty ranges based on an evaluation of the literature. These rate constants were then parametrized in the normalized form:

$$X_j = \frac{\ln\frac{k_j}{k_{j,0}}}{\ln s_j} \qquad j = \text{ca, a, b, c, d}$$

where $k_j$ are the variable rate coefficients of reactions ca, a, b, c, and d, $k_{j,0}$ are the rate coefficients of these reactions at the central point, and $s_j = (k_{max}/k_{min})^{1/2}$ is the span (allowed range) of the $j$ rate coefficient. Because these experiments cover a range of temperature, the $X$ variables are the $A$ factors, activation energies, and $T^n$ exponents of the five rate constants.

We wish to derive the best set of $X$ values to describe the entire ensemble of data and use a systematic optimization technique to do so. This technique involves first fitting the computed (model) values of the times to one-quarter and three-quarters of the maximum concentration to a second-order polynomial, the "response surface", for each experiment $m$:

$$t_m = b_{0,m} + \sum_{i=1}^{5} b_{i,m}X_i + \sum_{i=1}^{5}\sum_{i\le j}^{5} b_{ij,m}X_iX_j, \quad m = {}^1/_4, {}^3/_4$$

The coefficients of the polynomial are obtained from a regression analysis with respect to the $X$'s on the calculations performed according to a central composite factorial design. Values of the observables computed using this polynomial representation can then be compared to the "target" experimental values, allowing the $X$'s to assume any value within the predetermined error bounds. An objective function is constructed which computes the total error or deviation between the OH data set and the model representation. Here, $\Phi = \sum[1 - \Delta t(\text{calc})/\Delta t(\text{exp})]^2$, summed over 19 representative experiments from the five sets, for both OH and CO data. By mathematically minimizing this function via a computerized search routine, the best rate constant set representation ($X$'s) of the data is determined. Often, as was the case here, some of the $X$ variables will be constrained. The free optimization gives results for OH + $H_2$, for example, that are low and inconsistent with recent literature data. Thus, we conducted a series of constrained optimizations using various combinations of literature rate expressions for $k(a-d)$, and selected the minimum error result.

Details of the experiments and the data reduction can be found in the thesis of C.-L. Yu.[18]

## Results

**OH + CO.** The rate coefficient at 293 K for the OH + CO reaction as a function of helium pressure is presented in Figure 1a. The data were observed to be in general agreement with previous studies performed in the same pressure range, but are more precise.

The high-temperature value found in the shock tube experiments can be represented by $k_{ca} = 4.76 \times 10^7 T^{1.228} e^{-35/T}$ cm$^3$ mol$^{-1}$ s$^{-1}$. The optimization run producing this result uses the rate constants of Yu et al.[19] for $k_a$, Sutherland et al.[20] for $k_b$, Michael and Sutherland[21] for $k_c$, and Wooldridge et al.[22a] for $k_d$. The CO shock tube results alone would give $k_{ca} = 1.01 \times 10^7 T^{1.404} e^{359/T}$ cm$^3$ mol$^{-1}$ s$^{-1}$. Because the data fitting optimization relies in the end on selected literature expressions for the

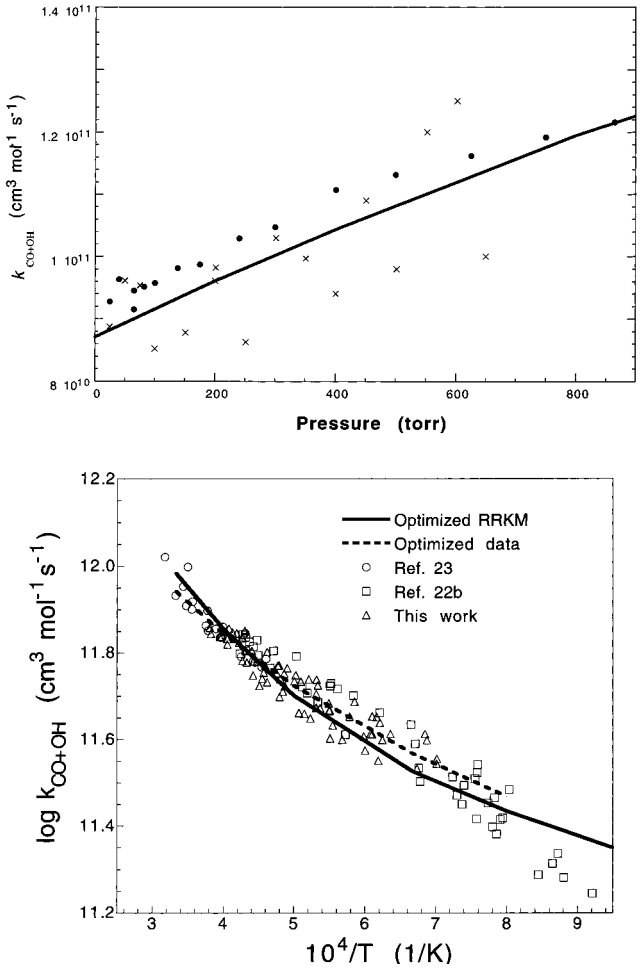


**Figure 1.** (a, top) Rate constant data for OH + CO + He at 293−298 K (dots are this work, × is ref 24). Solid line is the optimized RRKM fit with $\langle \Delta E \rangle = 0.15$ kcal/mol. (b, bottom) Recent rate constant data for OH + CO at high temperatures. Triangles and dashed line are this work. Solid line is the optimized theory.

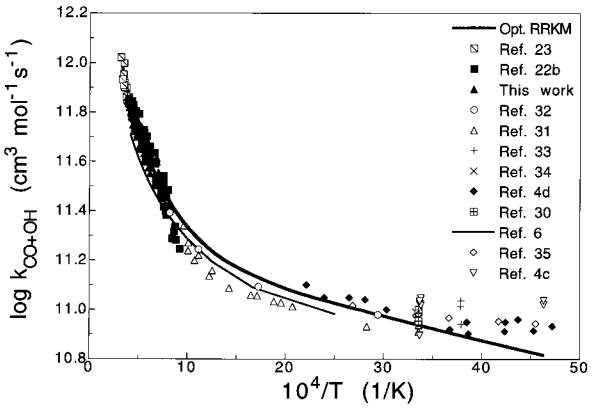


**Figure 2.** Temperature-dependent data and optimized RRKM results for OH + CO → H + $CO_2$.

other sensitive rate constants, we can extract individual rate constants from each experimental measurement. These are given in the last column of Table 1, and shown in Figure 1b along with other selected recent high-temperature results.[22b,23] Good consistency is observed. Figure 2 summarizes much of the low-pressure data for OH + CO over the wider temperature range, including the current results.

**OD + CO.** The data obtained herein for the pressure-dependent rate constants of OD + CO in several bath gases at 298K are shown in Figure 3a. The relative efficiencies are

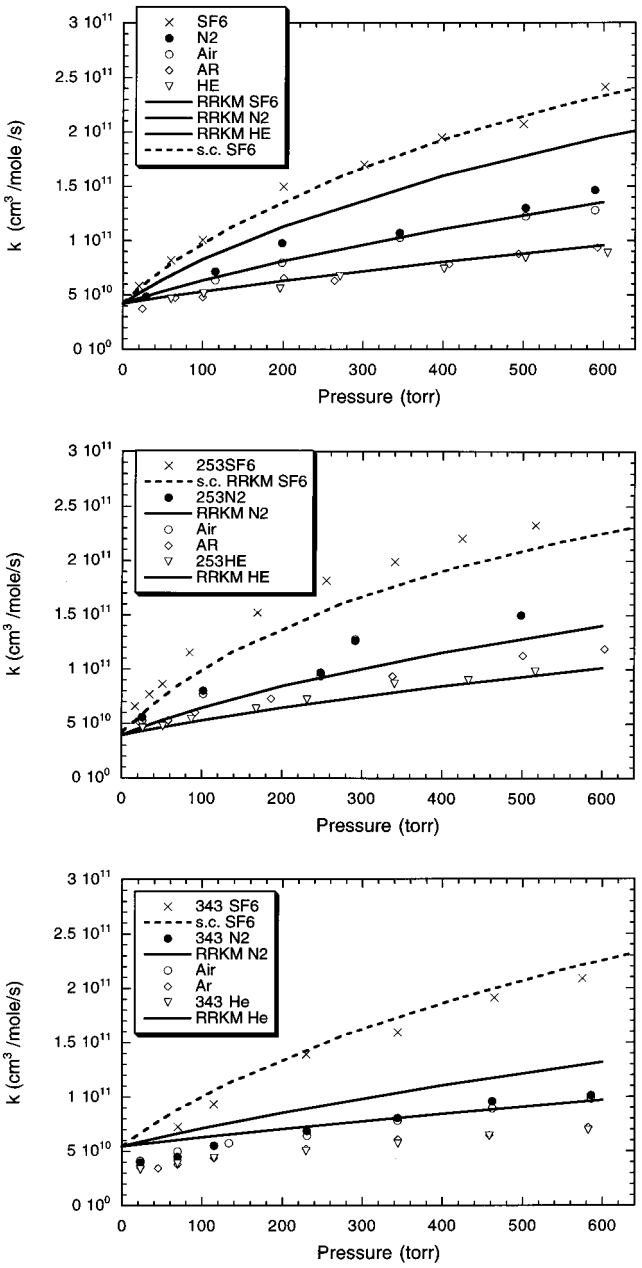


**Figure 3.** (a, top) Pressure-dependent rate data and RRKM fits for OD + CO in various bath gases at 298 K. RRKM fits shown for He, $N_2$, $SF_6$, and strong collision $SF_6$ (dashed line). (b, middle) Results at 253 K. (c, bottom) Results at 343 K.

as expected, and air and nitrogen are nearly identical. In helium there is good agreement compared to the results of Paraskevopoulos and Irwin.[24] In nitrogen and $SF_6$ a greater pressure dependence than previously reported[24] is observed. There are no previous data at other temperatures. In Figure 3b,c, we plot the pressure dependent results at 253 and 343 K.

## Optimization of Theory

**Methodology.** *General.* The use of solution mapping methodology to extract the best value from the data of the rate constant $k_{ca}$ was described earlier. In a completely analogous manner, the measured values of the rate constants, including their temperature and pressure variation, have been employed to extract optimized parameters of the PES. In this case, the response surface was based on RRKM calculations and the targets are various experimental measurements.

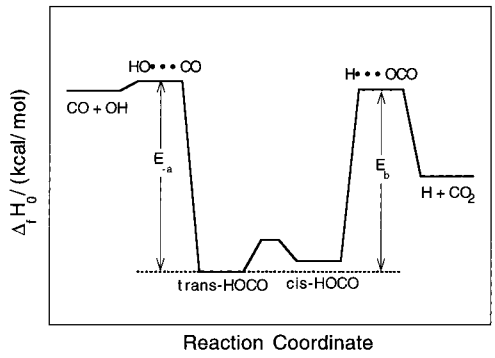


**Figure 4.** Potential energy surface for the HOCO system.

*Specific Application to H(D)OCO System.* The general features of the PES for this system are well agreed upon. Figure 4 shows a sketch of the reaction path profile through the surface with zero-point energies included. The two transition states were found to lie at very close to the same energy and in fact their relative positions (including zero point energy) were found to switch between the HOCO and the DOCO system. Previous RRKM theory fits[1,2,4a,d,6] of experimental results have also shown nearly isoenergetic barriers.

The new data reported here on the pressure dependence of HO + CO and DO + CO, the high-temperature values of the rate constant in the HOCO system reported here and from other laboratories,[22b,23] and the very high pressure dependent rate data reported by Fulle et al.[1] should allow the extraction of the magnitude of these barriers and other key PES parameters with improved precision, using RRKM theory to model the reaction system. The other sensitive model/surface parameters include the nature of the reaction coordinate in the transition state involved in the HOCO → H + $CO_2$ reaction, multipliers used to modify the initial values of the transition state frequencies (see Table 2), and the average energy transferred in a collision with each bath gas partner.

We use repeated applications of RRKM theory, allowing the variation of these PES parameters within a predetermined span, to determine a "response surface" from a number of computer calculations guided by a factorial design. Each response surface is a polynomial representation of RRKM theory predictions of the OH(OD) + CO rate constant at a chosen experimental temperature, pressure, and isotope, as a function of the RRKM parameter variables. Optimization of the theoretically calculated rate constants to match the "target" experimental data is carried out by minimizing the objective function describing the differences between calculations and experiments.

We selected a range of representative experimental target values for the low-pressure $k_{ca}$ over the range of atmospheric and combustion temperatures to include in the RRKM optimization. These include results from this study or others consistent with it. (See references in Table 3.) In addition, with the new OD + CO rate measurements reported here, a selection of isotopic targets is also included.

High-pressure target values at 300 K for both isotopes were taken from refs 1 and 4a which measured the relaxation of OH or OD ($v = 1$) by CO. This leads to an excited HOCO that decomposes to ground-state OH rapidly; thus the formation of HOCO is rate limiting. See Fulle et al.[1] for a full discussion.

Both high- and low-pressure (i.e., chemical activation) rate constants, computed using a two-channel RRKM code at temperatures corresponding to the experimental values, are used to create the response surfaces and the objective function. The code is a revision[18] of that by Gilbert and Smith,[25] with a 1 $cm^{-1}$ resolution for precise results in this sensitive system. It sums over both $E$ and $J$. The barrier height parameters $E_1$ and $E_2$ were given a 3 kcal/mol range near values from our earlier work.[5,6] The initial vibrational frequencies for the transition states were taken as 90% of those computed by Schatz et al.[11] The lowest two frequencies for each transition state were adjustable (as pairs) by multipliers of 0.8−1.2 in the optimization. The HO−CO transition state internal rotor was assumed free. The H−OCO reaction coordinate provided a fifth variable, being allowed to vary between pure HO stretch and C−O−H bend. In this initial application of the RRKM optimization, we have not included a barrier to the HO−CO rotor or a tunneling probability as additional variables. Because only zero and infinite pressure targets are involved, the energy and structure of HOCO itself are immaterial to the optimization.

Since only the chemical activation and high-pressure experimental values (neither of which depends on pressure) were used as "targets", values of the collision efficiency and $\Delta E_x$, the average energy transferred in a collision with the bath molecule $x$, were extracted later by fitting the pressure-dependent data with a two-channel RRKM model using the optimized values of the barrier heights, frequencies and reaction coordinate for the H···OCO transition state.

Analytical expressions that fit the known data well and which may be used to predict values of the rate constants under as yet unexplored conditions were then formulated using these optimized PES parameters. Tables 2 and 3 contain the PES variables and the target data, as well as the results of the optimization.

In performing the RRKM computations, special attention must be given to three factors. (1) To take advantage of the OD data presented here, it is necessary to assign frequencies in the adduct and the transition states in a manner consistent with known isotope effects. (2) OH/OD thermochemistry must be calculated correctly, properly taking into account electronic levels and nonclassical rotations. State counting is required at low temperatures, and the JANAF values[26] used here are appropriately formulated. (Most RRKM codes are not sufficient since they do not treat the effect of electronic states on thermochemistry.) (3) The near equivalence of the barrier heights requires high-precision RRKM computations. The calculations reported here sum over both $E$ and $J$ and use small grain (1 $cm^{-1}$) and step (10 $cm^{-1}$) size. Values of the high-pressure rate constants calculated for each reaction channel were compared with values computed from simple transition state theory to check for convergence of the RRKM computations.

**Results.** *Low Pressure (Chemical Activation) and High Pressure*. The input data required to compute the first-order approximation to the chemical activation and high-pressure limit rate constants can be found in the literature. Ab initio calculations[11] of the surface are the starting point, but there is also experimental data on the heat of formation[27] of HOCO and some of its vibrational frequencies.[28] The molecular parameters employed are listed in Table 2.

The experimental data that were used as targets and weighting factors associated with each are shown in Table 3 along with the values computed with the RRKM code using optimized values of the parameters. The percentage error for each target value and the least-squares error for the entire fit are also shown. The value of the chemical activation rate constant at 300 K was heavily weighted given the large database for this value.

Several optimization runs were performed. In some, weighting was varied, and in others, constraints were placed on some of the variables. Attempts to force the reaction coordinate in

**TABLE 2: RRKM Parameters for the OH(OD) + CO Reaction**

| | adduct | transition states | | adduct | transition states | |
|---|---|---|---|---|---|---|
| | HOCO[a] | {HO···CO}‡ | {H···$CO_2$}‡ | DOCO[a] | {DO···CO}‡ | {D···$CO_2$}‡ |
| vibrational frequencies ($cm^{-1}$) | 3603 | 3480[b] | 2100[b] | 2660 | 2568[b] | 2100[b] |
| | 1844 | 1990[b] | 1260[b] | 1842 | 1990[b] | 1260[b] |
| | 1211 | 972[c] | 1032[c] | 1093 | 700[b,c] | 744[b,c] |
| | 1065 | 354[c] | 540[c] | 870 | 354[b,c] | 420[b,c] |
| | 615 | | 1605[c] | 609 | | 1288[c] |
| | 515 | | | 396 | | |
| inactive rotational constant ($cm^{-1}$)[d] | 0.369 (1,2) | 0.253 (1,2) | 0.357 (1,2) | 0.345 (1,2) | 0.237 (1,2) | 0.323 (1,2) |
| active rotational constant ($cm^{-1}$)[d] | 5.60 (1,1) | 4.40 (1,1) | 4.76 (1,1) | 5.17 (1,1) | 4.03 (1,1) | 4.04 (1,1) |
| | | 29.1 (1,1)[e] | | | 19.6 (1,1)[e] | |
| $\Delta H°_{f,0}$ (kcal/mol) | −52.5 | | | −53.576 | | |
| $\Delta H^{‡}_0$ (kcal/mol) (relative to H(D)OCO) | | 35.545[c] | 35.080[c] | | 35.834[c] | 36.021[c] |

[a] Vibrational frequencies were taken from Jacox.[28b] Rotational constants are those of Radford et al.[28c] $\Delta H°_{f,0}$ was that reported by Rusic et al.[27] [b] Data are *ab initio* values of Schatz et al.[11] multiplied by 0.9. [c] Optimized parameters (see text). [d] Quantities in parentheses are symmetry number and dimension, in that order. [e] Torsional vibration was treated as a free rotor.

**TABLE 3: Targets for the RRKM Optimization.**

| H/D | $T$ (K) | $P$ | wt | experimental target[a] | optimization error | ref |
|---|---|---|---|---|---|---|
| H | 216 | 0 | 1 | 7.50E10 | −0.126 | 4d |
| H | 250 | 0 | 1 | 7.50E10 | −0.001 | 31 |
| H | 300 | 0 | 10 | 9.00E10 | −0.032 | 30 |
| H | 300 | ∞ | 1 | 6.00E11 | −0.059 | 4a |
| H | 511 | 0 | 1 | 1.066E11 | +0.153 | 31 |
| H | 800 | 0 | 1 | 1.44E11 | +0.172 | 31 |
| H | 1040 | 0 | 1 | 2.186E11 | +0.006 | 31 |
| H | 1250 | 0 | 1 | 2.59E11 | +0.050 | 22b |
| H | 1500 | 0 | 1 | 3.72E11 | −0.096 | this work |
| H | 2000 | 0 | 1 | 5.24E11 | −0.041 | this work |
| H | 2500 | 0 | 1 | 6.90E11 | +0.038 | this work |
| H | 3000 | 0 | 1 | 9.26E11 | +0.039 | 23 |
| D | 216 | 0 | 1 | 3.10E10 | −0.168 | 4c |
| D | 278 | 0 | 1 | 3.50E10 | +0.074 | this work |
| D | 300 | 0 | 3 | 4.00E10 | +0.053 | this work |
| D | 300 | ∞ | 3 | 5.72E11 | +0.087 | 4a |

[a] $xEn \equiv x \times 10^n$.

the H···OCO transition state to be purely the O−H stretch consistently degraded the fit. This is largely a function of the isotopic data. The low-pressure OD + CO data is required to determine this parameter. It is also clearly not legitimate to independently vary the OD + CO energies or frequencies to separately fit the isotopic results, as they are functions of the same force constants and potential energy surface.

As seen in Figures 3 and 5, a good match is found to most of the target data by the optimized RRKM parameters. Small but significant deviations are only found in the intermediate (500−1000 K) temperature range where the upward curvature observed for the chemical activation rate constant is overpredicted, and at the low temperatures where a sizable decline is erroneously forecast. (Potential targets at temperatures below 200 K were omitted as a result.) Additional weighting in the optimization on these missed targets did not improve the match significantly, and flattening out this predicted curvature is a fundamental problem for any RRKM approach correctly exploring this parameter space, given the real energy barrier to HOCO formation from HO + CO (which arises from the $k$ target) and will force a temperature dependence.

*Pressure Dependence*. Having established the transition state parameters, the pressure-dependent data was fit by calculations using the two-channel RRKM code (including a Waage−Rabinovitch correction factor[29] of 1.4 for the HO(DO)···CO transition state) and the modified strong collision approach of Troe,[7] in which the collision efficiency, $\beta_x$, is related to the

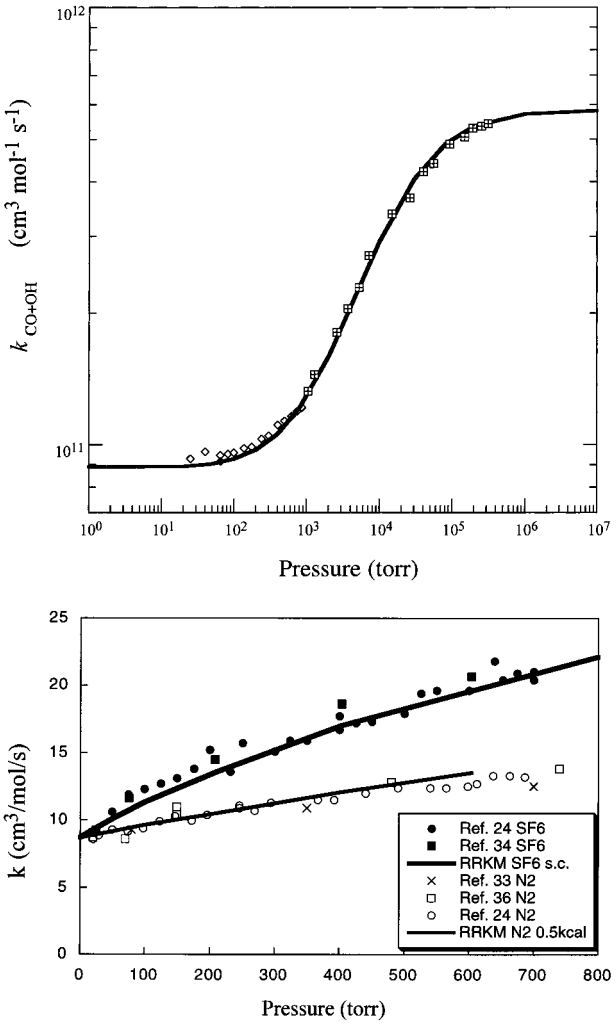


**Figure 5.** (a, top) Pressure-dependent rate constants for OH + CO in He at 298 K: squares, ref 1; diamonds, this work; solid line is the optimized RRKM result. (b, bottom) Literature data and RRKM results for OH + CO at 298 K at various $SF_6$ and $N_2$ bath gas pressures.

average energy transferred per collision with bath gas $x$, by

$$\frac{\Delta E}{F_E kT} = \frac{\beta_x}{(1-\beta_x^{1/2})}$$

where $F_E$ is the energy dependence of the density of states.

The values of $\Delta E_x$ needed to fit the pressure-dependent data are 0.15 kcal/mol for He and 0.6 kcal/mol for $N_2$, in reasonable

**TABLE 4: Optimized Parameters from Two-Channel RRKM Calculations for OH (OD) + CO + $N_2$**

$k(\mathrm{sc}) = 10^{a} T^{b} \mathrm{e}^{-c/T}$
$F_c(\mathrm{sc}) = a\mathrm{e}^{-b/T} + \mathrm{e}^{-T/c}$
$K = 10^{a} T^{b} \mathrm{e}^{-c/T}$
$k_0(\mathrm{wc}) = \beta k_0(\mathrm{sc})$; $k_\infty^{\mathrm{ca}}(\mathrm{wc}) = k_\infty^{\mathrm{ca}}(\mathrm{sc})/\beta$; $F_c(\mathrm{wc}) = \beta^{.14} F_c(\mathrm{sc})$; $\beta = 72.375T^{-0.9155}$

(a) Unimolecular Reactions

| | $(k_0/[\mathrm{M}])/\mathrm{cm^3\ mol^{-1}\ s^{-1}}$ | | | $k_\infty/\mathrm{s^{-1}}$ | | | $F_c$ | | |
|---|---|---|---|---|---|---|---|---|---|
| | **a** | **b** | **c** | **a** | **b** | **c** | **a** | **b** | **c** |
| HOCO → OH + CO | 25.137 | −2.396 | 18862 | 14.074 | 0.132 | 18349 | 0.729 | 513 | 540 |
| DOCO → OD + CO | 26.171 | −2.678 | 18979 | 14.363 | 0.041 | 18492 | 0.693 | 431 | 409 |
| HOCO → H + $CO_2$ | 26.775 | −3.148 | 18629 | 11.915 | 0.413 | 17783 | 1.049 | 2407 | 823 |
| DOCO → D + $CO_2$ | 24.782 | −2.614 | 18996 | 12.093 | 0.394 | 18278 | 1.460 | 3418 | 1709 |

(b) Chemical Activation Process

| | $k_0^{\mathrm{ca}}/\mathrm{cm^3\ mol^{-1}\ s^{-1}}$ | | | $[\mathrm{M}]k_\infty^{\mathrm{ca}}/\mathrm{s^{-1}}$ | | | $F_c$ | | |
|---|---|---|---|---|---|---|---|---|---|
| | **a** | **b** | **c** | **a** | **b** | **c** | **a** | **b** | **c** |
| OH + CO → H + $CO_2$ | 6.882 | 1.444 | −301 | −3.043 | 3.848 | −480 | 1.209 | 1560 | 1568 |
| OD + CO → D + $CO_2$ | 6.801 | 1.458 | −131 | −4.679 | 4.290 | −522 | 0.862 | 2950 | 5490 |

(c) Equilibrium Constant

| | $K/\mathrm{mol\ cm^{-3}}$ | | |
|---|---|---|---|
| | **a** | **b** | **c** |
| HOCO = OH + CO | 4.897 | −0.968 | 18234 |
| DOCO = OD + CO | 5.677 | −1.190 | 18505 |
| HOCO = H + $CO_2$ | −0.837 | 0.026 | 5398 |
| DOCO = D + $CO_2$ | 0.432 | −0.311 | 6447 |
| OH + CO = H + $CO_2$ | −5.734 | 0.993 | −12836 |
| OD + CO = D + CO2 | −5.245 | 0.879 | −12058 |

agreement with values extracted from other systems.[30] High $\beta$ values, near the strong collision limit, were needed to fit the $SF_6$ data, but need not be considered anomalous considering ~20% uncertainties in collision cross sections and the neglect of anharmonicity effects of up to 50% in the state density integral term that enters into the $k_0$ calculation. The pressure-dependent results are only weakly sensitive to the binding energies and frequencies of the HOCO adduct.

Note that no adjustment to $\Delta E_x$ is permitted or needed between isotopic systems. The shape of the falloff is largely governed by this one parameter. The increase in the association reaction and decrease in the chemical activation channel with pressure are both accommodated. The resulting fits to the pressure-dependent data of this study are illustrated in Figures 1 and 3. The fits, which show little temperature dependence, tend to overpredict $k$ at 343 K and underpredict $k$ at 253 K, by up to 20%. The wide range of pressure-dependent data[1] in helium at 298 K is also well matched, as shown in Figure 5a. The theory consistently deviates from similar results at other temperatures (−30% at 190 K, −15% at 250 K, +15% at 400 K, and +40% at 500−800 K), probably from its inability to produce a flat temperature dependence over this range. Figure 5b shows the 298 K match to literature data for OH + CO in $N_2$ and $SF_6$ bath gas, using the same parameters that achieved the equally good fit of the OD + CO data shown in Figure 3a−c.

## Conclusions

**Recommended Expression.** The large body of data considered here can be represented by the expressions in Table 4. These expressions are based on a realistic PES for this system and should allow extrapolation outside of the current experimental limits. (The fitting procedure that produces these expressions over such a wide temperature range may introduce an "error" with respect to the RRKM calculations that we estimate to be about 5% into the rate constant values.)

**Higher Levels of Theory?** It may be possible to improve the fit to the data. The pressure dependence may be treated using a master equation instead of the modified strong collision approach. A polynomial defining the response surface can be constructed with seven sensitive variables rather than five. Some calculations were performed where the torsional motion in the HO···CO transition state that is treated as a free rotor was changed to a hindered rotor, with the barrier to rotation as an optimization variable. The results were sensitive to this variable and the fit was improved. However, the improvement is really quite within the uncertainty of the target data, so the five-variable fit was kept.

There have been reports[4c] claiming that a higher barrier for the channel leading from H(D)OCO to products along with a tunneling correction can fit the data. We find that the surface described by our optimized parameters requires no tunneling correction. This is based on Eckart calculations[18] and is to be expected when the exit barrier is at or below the entrance channel energy (in our case), and is consistent with other similar representations.[1] However, it is clearly not possible to fit the low-temperature chemical activation data without an approach that employs tunneling, given that the high-pressure rate constants mandate an entrance barrier for this reaction. Thus, a future RRKM optimization will include tunneling, using a PES with a barrier to H + $CO_2$ formation that is higher than the barrier for HOCO formation from OH + CO. An Eckart potential frequency will be employed with the appropriate isotope effect as an additional parameter, to explore further this possibility. We will incorporate additional targets, including laser experiments purporting to measure lifetimes of excited HOCO complexes. High-temperature shock tube results for the OD + CO system could also be useful.

**Acknowledgment.** It is a pleasure to dedicate this paper to Sidney Benson on the occasion of his 80th birthday. All the authors owe Sidney thanks for his great contributions to our

science. D.M.G. in particular salutes his mentor! This work was supported by the Basic Sciences Group of the Gas Research Institute (SRI and UCB), the U.S. Department of Energy Office of Basic Energy Science (Sandia), and the Climate and Global Change Research Program (NOAA).

**Supporting Information Available:** Tables of rate coefficients for the HO + CO and OD + CO reactions (5 pages). Ordering information is given on any current masthead page.

## References and Notes

(1) Fulle, D.; Hartman, H. F.; Hippler, H.; Troe, J. *J. Chem. Phys.* **1996**, *105*, 983.

(2) Mozurkewich, M.; Lamb, J. J.; Benson, S. W. *J. Phys. Chem.* **1983**, *88*, 6435.

(3) Dryer, F.; Naegeli, D.; Glassman, I. *Combust. Flame* **1971**, *17*, 270.

(4) (a) Brunning, J.; Derbyshire, R. W.; Smith, I. W. M.; Williams, M. D. *J. Chem. Soc., Faraday Trans. 2* **1988**, *84*, 105. (b) Frost, M. J.; Sharkey, P.; Smith, I. W. M. *Faraday Discuss. Chem. Soc.* **1991**, *91*, 305. (c) Frost, M. J.; Sharkey, P.; Smith, I. W. M. *J. Phys. Chem.* **1993**, *97*, 12254. (d) Smith, I. W. M.; Zellner, R. *J. Chem. Soc., Faraday Trans. 2* **1973**, *69*, 1617.

(5) Golden, D. M. *J. Phys. Chem.* **1979**, *83*, 108.

(6) Larson, C. W.; Stewart, P. H.; Golden, D. M. *Int. J. Chem. Kinet.* **1988**, *20*, 27.

(7) Troe, J. *J. Chem. Phys.* **1977**, *66*, 4745.

(8) Frenklach, M. *In Combustion Chemistry*; Gardiner, W. C., Jr., Ed.; Springer-Verlag: New York, 1984; Chapter 7.

(9) Miller, D.; Frenklach, M. *Int. J. Chem. Kinet.* **1983**, *15*, 677.

(10) Frenklach, M.; Wang, H.; Rabinowitz, M. J. *Prog. Energy Combust. Sci.* **1992**, *18*, 47.

(11) Schatz, G. C.; Fitzcharles, M. S.; Harding, L. B. *Faraday Discuss. Chem. Soc.* **1987**, *84*, 359.

(12) Tully, F. P.; Goldsmith, J. E. M. *Chem. Phys. Lett.* **1985**, *116*, 345.

(13) Tully, F. P.; Droege, A. T.; Koszykowski, M. L.; Melius, C. F. *J. Phys. Chem.* **1986**, *90*, 691.

(14) Vaghjiani, G. L.; Ravishankara, A. R. *J. Phys. Chem.* **1989**, *93*, 1948.

(15) Yu, C.-L.; Wang, C.; Frenklach, M. J. *J. Phys. Chem.* **1995**, *99*, 14377.

(16) Yuan, T.; Wang, C.; Yu, C.-L.; Frenklach, M.; Rabinowitz, M. *J. Phys. Chem.* **1991**, *95*, 1258.

(17) Frenklach, M.; Wang, H.; Goldenberg, M.; Smith, G. P.; Golden, D. M.; Bowman, C. T.; Hanson, R. K.; Gardiner, W. C.; Lissianski, V. *GRI-Mech—An Optimized Detailed Chemical Reaction Mechanism for Methane Combustion*; Gas Research Institute Report GRI-950058, 1995.

(18) Yu, C.-L. Ph.D. Thesis, Pennsylvania State University, 1995..

(19) Yu, C.-L.; Frenklach, M.; Masten, D. A.; Hanson, R. K.; Bowman, C. T. *J. Phys. Chem.* **1994**, *98*, 4770.

(20) Sutherland, J. W.; Michael, J. V.; Pirraglia, A. N.; Nesbitt, F. L.; Klemm, R. B. *Twenty-First Symposium (International) on Combustion [Proceedings]*; The Combustion Institute: Pittsburgh, PA, 1988; p 929.

(21) Michael, J.; Sutherland, J. W. *J. Phys. Chem.* **1988**, *92*, 3853.

(22) (a) Wooldridge, M. S.; Hanson, R. K.; Bowman, C. T. *Int. J. Chem. Kinet.* **1994**, *26*, 389. (b) Wooldridge, M. S.; Hanson, R. K.; Bowman, C. T. *Twenty-Fifth Symposium (International) on Combustion [Proceedings]*; The Combustion Institute: Pittsburgh, PA, 1994; p 741.

(23) Lissianski, V.; Yang, H.; Qin, Z.; Mueller, M. R.; Shin, K. S.; Gardiner, W. C., Jr. *Chem. Phys. Lett.* **1995**, *240*, 57.

(24) (a) Paraskevopoulos, G.; Irwin, R. S. *Chem. Phys. Lett.* **1982**, *93*, 138. (b) Paraskevopoulos, G.; Irwin, R. S. *J. Chem. Phys.* **1984**, *80*, 259.

(25) Gilbert, R. G.; Smith, S. C. *Theory of Unimolecular and Recombination Reactions*; Blackwell: Oxford, UK, 1990.

(26) Chase, N. W.; Davies, C. A.; Downey, J. R.; Frurip, D. J.; McDonald, R. A.; Syverud, A. N. *J. Phys. Chem. Ref. Data* **1985**, *14* (Suppl. 1).

(27) Ruscic, B.; Schwarz, M.; Berkowitz, J. *J. Chem. Phys.* **1989**, *91*, 6780.

(28) (a) Jacox, M. E. *J. Phys. Chem. Ref. Data* **1988**, *17*, 269. (b) Jacox, M. E. *J. Chem. Phys.* **1988**, *88*, 6409. (c) Radford, H. E.; Wei, W.; Sears, T. J. *J. Chem. Phys.* **1992**, *97*, 3989.

(29) Waage, E. V.; Rabinovitch, B. S. *Chem. Rev.* **1970**, *70*, 377.

(30) DeMore, W. B.; Sander, S. P.; Golden, D. M.; Hampson, R. F.; Kinylo, M. J.; Howard, C. J.; Ravishamkara, A. R.; Kolb, C. E.; Molina, M. J. *Chemical Kinetics and Photochemical Data for use in Stratospheric Modeling*; NASA JPL Publication 97-4, 1997.

(31) Ravishankara, A. R.; Thompson, R. L. *Chem. Phys. Lett.* **1983**, 99, 377.

(32) Beno, M. F.; Jonah, C. D.; Mulac, W. A. *Int. J. Chem. Kinet.* **1985**, 17, 1091.

(33) Hynes, A. J.; Wine, P. H.; Ravishankara, A. R. *J. Geophys. Res.* **1986**, 91, 11815.

(34) Perry, R. A.; Atkinson, R.; Pitts, J. N. *J. Chem. Phys.* **1977**, 61, 5577.

(35) Davis, D. D.; Fisher, S.; Schiff R. J. *J. Chem. Phys.* **1974**, 61, 2213.

(36) Hofzumahaus, A.; Stuhl F. *Ber Bunsen-Ges. Phys. Chem.* **1984**, 88, 557.